

# Dislocation Evolution During Plastic Deformation: Equations vs. Discrete Dislocation Simulations

Kamyar M. Davoudi, Joost J. Vlassak

*School of Engineering and Applied Sciences, Harvard University, Cambridge, MA  
02138, USA*

## Abstract

Explaining the work hardening behavior of metals has been a big challenge over the past eighty years. Although individual processes are well understood, the study of the overall effects of these processes was difficult before the emergence of computer modeling. In this paper, we employ discrete dislocation dynamics to establish a continuum-based model for the evolution of the dislocation structure in polycrystalline thin films. The Taylor equation is evaluated and expressions are developed for the density of active dislocation sources, as well as dislocation nucleation and annihilation rates. We demonstrate how the size effect naturally enters the evolution equation. Very good agreement between the simulation and the model results is obtained. The current approach is based on a two-dimensional discrete dislocation dynamics model, but can be extended to three-dimensional models.

## Keywords

Dislocation Evolution — Nucleation Rate — Annihilation Rate — Density of Active Sources — Taylor Equation — Size Effect — Discrete Dislocation Dynamics

## 1 Introduction

“It is sometimes said that the turbulent flow of fluids is the most difficult remaining problem in classical physics. Not so. Work hardening is worse”, remarked Cottrell (2002). Work hardening, a mechanism that occurs in crystalline metals, manifests as a rise in the stress required for continued plastic deformation. Despite all the efforts that have been put toward the study of work hardening in the past 80 years, there is currently no generally accepted theory explaining all aspects of it (Kubin et al., 2009); finding a theory of work hardening is now as hopeless as ever, and research is aimed at establishing a model instead (Kocks and Mecking, 2003).

The first attempt to link the shear strength of a material to its microstructure was made by Taylor (1934). He recognized that the (athermal) flow stress is proportional to the square root of the dislocation density. Successive attempts were made by Friedel (1955), Seeger et al. (1955, 1957, 1963), Hirsch (1959), Hirsch and Mitchell (1967), Nabarro et al. (1964), and Kuhlmann-Wilsdorf (1962, 1985), just to name a few. Kocks, Mecking, Estrin, and their co-workers (1975, 1976, 1980, 1981, 1984, 1996) reached a milestone by integrating the physical and phenomenological

approaches. In their approach, a kinetic equation relates the flow stress  $\sigma$  to the plastic strain rate  $\dot{\epsilon}_p$ , the absolute temperature  $T$ , and the current microstructure. If there were no abrupt changes in the strain rate or the stress, a single structure parameter such as the dislocation density or the flow stress at a reference condition, was deemed sufficient to describe the structure (Estrin and Mecking, 1984). In some cases, such as upon stress reversals, two or more governing parameters were required (Mecking and Kocks, 1981; Turner, 1979). As the structure parameter varies during plastic deformation, that kinetic equation needs to be complemented with an evolution equation to fully describe the rate dependent plastic (viscoplastic) response of a material. This evolution equation describes the variation of the current structure parameter with plastic strain at given strain rate and temperature (Estrin and Mecking, 1984). Using this formulation Kocks et al. were able to successfully calculate the saturation stress for different loading rates, the steady-state creep at constant stress or constant load, and the hardening rate ((Estrin, 1996) and references therein).

A strong size-dependence, observed in many thin-film experiments, further complicated the construction of a work hardening theory. Several experiments (Doerner and Nix, 1986; De Guzman et al., 1993; Stelmashenko et al., 1993; Fleck et al., 1994; Lloyd, 1994; Ma and Clarke, 1995; McElhaney et al., 1998; Poole et al., 1996; Stölken and Evans, 1998; Uchic et al., 2004; Xiang and Vlassak, 2006) revealed that single crystalline or polycrystalline materials at the micro or nano-scale often support stresses that they could not possibly support in bulk form. These observations led to the mantra of “smaller is stronger”. The size effect was not a new phenomenon. Hall (1951) and Petch (1953), for example, showed in the 1950s that the strength of crystalline materials is strongly impacted by the grain size, and Estrin and Mecking (1984) considered the case of fine-grained materials in their evolution equation. However, the advent of the microelectronics industry and the use of thin metal films in small devices have brought about a new level of attention to the concept of size dependence. A detailed and quantitative understanding of the various size effects is essential for an effective and reliable design of these types of devices. Many of the failure mechanisms in micro-devices are stress-driven or otherwise mechanical in nature — delamination of coatings, stress voiding, and hillocking are just a few examples.

Plasticity in thin films originates from the same fundamental mechanisms observed in bulk materials and thus cannot be formulated without significant understanding of collective dislocation motion (Miguel et al., 2001). Although individual dislocation processes have been well studied, describing the ensemble behavior of dislocations has been challenging without computer modeling. In addition, computer simulations make it possible to investigate the contributions of different mechanisms by ruling out other factors.

Of the various computer simulation techniques, discrete dislocation dynamics (DDD) is the most suitable method to model thin films at the micron scale and below. In this method, the material is modeled as a continuum that contains dislocations. Grain boundaries may also be included for polycrystalline materials. Dislocations nucleate, move and are destroyed under a few simple constitutive laws. Three-dimensional DDD models capture the physics of problems accurately, but they are computationally demanding and are not easily applied to thin films. Therefore, most three-dimensional models are limited to single crystals, very small strains, small volumes of material, and low dislocation densities. For example, ParaDis, a powerful three-dimensional DDD code, which was originally developed at the Lawrence Livermore National Laboratory, can only model single-crystal materials. Two-dimensional discrete dislocation dynamics models, on the other hand, can model polycrystalline materials, realistic dislocation densities, and relatively large strains with much less computational effort. While these models necessarily miss some of the physics, recent studies have shown that two- and three-dimensional simulations can predict remarkably similar results in some cases (Ispánovity et al., 2013, 2010). Both types of simulations have been employed to study a range of phenomena including the effect of passivation layers on plastic flow in thin films (Davoudi et al., 2012; Nicola et al., 2006), the Bauschinger effect (Nicola et al., 2006; Shishvan et al., 2010; Danas and Deshpande, 2013; Lee et al., 2013; Davoudi et al., 2014), the effect of dislocation acceleration (Roos et al., 2001), the validity of the Taylor equation (Gómez-García et al., 2006; Devincre et al., 2008; Guruprasad and Benzerga, 2008; Madec et al., 2002; Sauzay and Kubin, 2011), the effects of dislocation sources and grain boundaries (Kumar et al., 2009), and the elastic anisotropy on the deformation of polycrystals (Shishvan et al., 2011), uniaxial deformation of micro- and nano-pillars (Greer et al., 2008; El-Awady et al., 2011; Ryu et al., 2013), fracture ((Van der Giessen, 2010) and the references therein), and multiscale modeling (Devincre et al., 2008; Groh et al., 2009).

Plastic deformation is path dependent; dislocation density cannot be determined by equilibrium thermodynamics. Plastic deformation is an irreversible, highly dissipative process that occurs far from equilibrium (Kubin and Canova, 1992; Sauzay and Kubin, 2011); thermodynamic extremum principles are not applicable (Hillert and Ågren, 2006; Sauzay and Kubin, 2011). Thus dynamic evolution equations for the dislocation structure and kinetic equations are required to model plastic flow (Sauzay and Kubin, 2011). Although many evolution equations have been developed (Kocks et al., 1975; Mecking and Kocks, 1981; Walgraef and Aifantis, 1985a, 1985b, 1985c; Aifantis, 1986; Follansbee and Kocks, 1988; Hähner, 1996a, 1996b; Nix and Lee, 2011) for materials in bulk form, there have been few attempts to use discrete dislocation simulations to check the validity of these equations. Devincre et al. (2008) have used discrete dislocation simulations to express the mean free path in terms of the critical shear stress, elastic moduli, density of junctions, and the number of active

slip planes. Ryu et al. (2013) presented a simple dislocation kinetics model for body-centered cubic micropillars under compression, and compared the results with the DDD results, demonstrating that the model was not completely successful in describing the dislocation evolution. In this paper, we derive a continuum model for the dislocation evolution in polycrystalline thin films that are passivated on both surfaces and use discrete dislocation simulations to verify the model. While in most DDD analyses edge dislocations can only glide, dislocations in this study are allowed to both glide and climb. Dislocation climb is a mechanism by which edge dislocations trapped at glide barriers can leave their primary slip planes. Thus climb acts as a softening process and may be taken as representative of a range of softening mechanisms that occur in a material.

The paper is organized as follows; first the framework of the two-dimensional DDD model is briefly described. Then we review the Taylor relation and derive an expression for the density of active dislocation sources. The next sections are devoted to deriving expressions for dislocation nucleation and annihilation. Combining these relations, a governing equation for the dislocation evolution is derived in the final section.

## 2 Methods

In discrete dislocation dynamics, a material is modeled as an elastic solid containing dislocations. Simulations are then carried out in an incremental fashion. At a given instant of time, it is assumed that the material is in equilibrium and that the displacement and stress fields are known. An increment of strain is prescribed and the positions of the dislocations in the material, the displacement field, and the stress field are updated using the following procedure: (1) The Peach-Koehler force on each dislocation is calculated; (2) in response to the Peach-Koehler forces, the dislocation structure evolves: dislocations move, new dislocations nucleate, and others are annihilated; (3) the stress state in the solid is calculated for the updated dislocation arrangement. Steps 1 and 3 follow from elasticity; step 2 requires the formulation of constitutive rules for dislocation behavior. Determining the stress state at each time step requires the solution of an elastic boundary value problem. Here we use the framework developed by Van der Giessen and Needleman (1995), where the stress, strain, and displacement fields are written as the superposition of two fields: one field due to the dislocations in an infinite medium and an image field that enforces the boundary conditions (Van der Giessen and Needleman, 1995). For step 2, we follow the constitutive rules suggested by Kubin et al. (1992) for dislocation glide, dislocation annihilation and dislocation nucleation. When the local shear stress on a dislocation source inside the material exceeds the strength of the source during a specific time, the source emits a dislocation dipole. The distance between the two dislocations is taken such that the attraction between the two dislocations is balanced

by the source strength. When two dislocations of opposite sign come closer to each other than a critical distance, say  $6b$  where  $b$  is the magnitude of the Burgers vector, the dislocations annihilate each other and are removed from the model. At temperatures above 20 K, phonon drag is large enough to make dislocations quickly reach the overdamped regime (Kubin et al., 1992) and a linear relationship between the Peach-Koehler force on a dislocation and its glide velocity is assumed. Dislocation climb was implemented using the model described by Davoudi et al (2012).

Discrete dislocation dynamics simulations were performed for freestanding polycrystalline aluminum films passivated on both surfaces. The films were subjected to uniaxial tension as illustrated schematically in Fig. 1. Thin films of aluminum often have a columnar grain structure, which was modeled as a two-dimensional array of randomly oriented rectangular grains of thickness  $h$ , in line with Nicola et al. (Nicola et al., 2006). Each grain had three sets of slip planes that differed by  $60^\circ$  (Rice, 1987). The grain size of the film was  $1 \mu\text{m}$ , while the thickness of the passivation layers was taken to be 20 nm. The passivation layers were assumed to deform elastically and had the same elastic properties as the film material. Both grain boundaries and passivation layers were assumed impenetrable to dislocations. All simulations were performed at a temperature of 900 K. Periodic boundary conditions were applied at the left and right boundaries of the model. Plane strain conditions were assumed in the  $xy$ -plane; the tensile stress in the film was calculated as the stress  $\sigma_{xx}$  averaged over the thickness of the film.

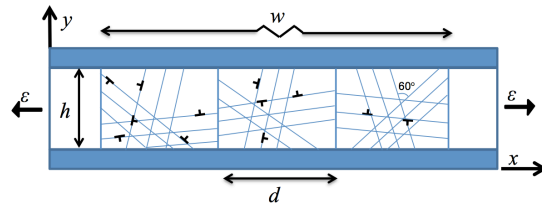


Figure 1: Schematic representation of the thin-film model

The films were initially dislocation free, but dislocation sources were randomly distributed on the slip planes. The density of dislocation sources was taken as  $15 \mu\text{m}^{-2}$  in all simulations. The strengths of the dislocation sources,  $\tau_{nuc}$ , were randomly selected from a Gaussian distribution with a mean of 100 MPa and a standard deviation of 20 MPa. To limit computation time, a high strain rate of  $4000 \text{ s}^{-1}$  was used in all simulations. The time step for climb was taken 100 times larger than the time step for glide. To reduce the effects of the initial conditions, four realizations of the model were run for each set of parameters. Realizations differed from each other with respect to grain orientations and locations of dislocation sources. The choice of parameters and the model are outlined in more detail in (Davoudi et al., 2012, 2014).

### 3 Taylor Equation

The Taylor equation was one of the first expressions relating the flow stress of a material to its dislocation density. The expression was first developed by G.I. Taylor (1934) in an attempt to describe work hardening. The equation arises naturally if one assumes the flow stress is the external stress required to drive two dislocations on parallel slip planes past one another. Given that the maximum shear stress associated with a dislocation is of order  $\mu b/r$ , where  $\mu$  is the shear modulus and  $r$  the distance to the dislocation, and that the average spacing between randomly distributed dislocations is of order  $1/\sqrt{\rho}$ , the flow stress  $\tau$  of a material can be written as

$$\tau = \tau_0 + \alpha\mu b\sqrt{\rho}. \quad (1)$$

In this expression,  $\alpha$  is a dimensionless parameter ranging from 0.05 to 2.6 for different materials (Lavrentev, 1980), and  $\tau_0$  is the flow stress of the material in the absence of dislocation interactions. In other words,  $\tau_0$  is the shear resistance to dislocation motion when  $\rho \approx 0$  (Lavrentev, 1980). Other work-hardening models lead to a similar linear relation between the flow stress and the square root of the dislocation density, but with different proportionality constants (Nabarro et al., 1964). It is convenient to rewrite Eq. (1) as in (Viguier, 2003)

$$\tau - \tau^* = \alpha\mu b\left(\sqrt{\rho} - \sqrt{\rho^*}\right), \quad (2)$$

where  $\tau^*$  and  $\rho^*$  are the flow stress and dislocation density at the point where the material first becomes fully plastic. Many experiments have shown that the Taylor equation holds true for f.c.c., b.c.c., and h.c.p metals, as well as for ionic and covalent materials (Viguier, 2003), both in single crystals and in polycrystals, as long as the flow stress is solely controlled by interactions between dislocations (Kocks and Mecking, 2003). Using the Taylor factor,  $M$ , which relates the shear flow stress  $\tau$  of a single crystal to the uniaxial flow stress  $\sigma$  of a polycrystal, the Taylor equation can be reformulated for the uniaxial loading of a polycrystal,

$$\sigma = \sigma^* + M\alpha\mu b\left(\sqrt{\rho} - \sqrt{\rho^*}\right). \quad (3)$$

In the absence of a crystallographic texture, the Taylor factor takes a value of 3.067 for f.c.c. and b.c.c. metals in tension or compression (Hull and Bacon, 2011; Kocks, 1970). The Taylor factor changes only slightly if the material has a texture (Xiang et al., 2004), and varies very slightly with deformation (Estrin, 1996). In our model, we have taken  $M = 3.10$ .

Figure 2 shows several stress-strain curves obtained for films with different thicknesses using DDD simulations. The solid lines represent the simulation results; the dashed lines represent the stress-strain curves derived from the Taylor model, Eq.

(3). The proportionality constant is determined by linear regression of  $\sigma - \sigma^*$  on  $M\mu b(\sqrt{\rho} - \sqrt{\rho^*})$ , where the stress and the dislocation density are known from the simulation results. The figure clearly illustrates that the Taylor equation provides a good fit to the simulation data for small strains ( $\epsilon < 0.7\%$ ), whether or not dislocation climb is enabled.

When dislocation climb is enabled, dislocations are more dispersed, and the average spacing between dislocations is larger than when dislocations can only glide. For this reason, the values of  $\alpha$  are smaller in Fig. 2b than in Fig. 2a. A large number of experimental observations indicate that  $\alpha$  decreases with increasing temperature (Kocks and Mecking, 2003). This decrease is attributed to the activation of recovery mechanisms such as cross slip and dislocation climb and to the dispersion of dislocations, in line with what is observed here.

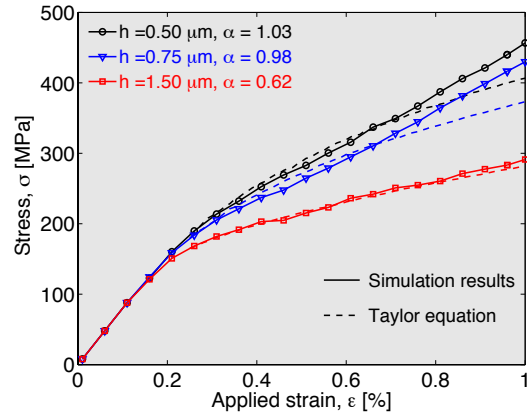
At larger strains, the agreement between the Taylor equation and the stress-strain curves in Fig. 2 is not as satisfying: the stress-strain curves derived from the simulations tend to show linear hardening, while the Taylor equation predicts parabolic hardening. This discrepancy can be attributed to the formation of dislocation pile-ups in the simulation. As plastic deformation proceeds, the number of dislocations in pile-ups increases and the number of dislocations is a linear function of the external stress (Leibfried, 1951; Hirth and Lothe, 1982).

When the dislocation structure is converted from a random distribution to an organized microstructure, Eq. (3) remains valid if  $\alpha$  is allowed to vary with  $\epsilon_p$ . For example, experiments on bulk materials have shown that  $\alpha$  decreases with increasing deformation when dislocation cells form inside the grains (Kocks and Mecking, 2003). The results in Fig. 2 suggest that pile-up formation in thin films may cause  $\alpha$  to increase with  $\epsilon_p$ . If  $\alpha$  varies with  $\epsilon_p$ , the work-hardening rate  $\theta_p$  of a polycrystalline metal can be written as

$$\theta_p \equiv \frac{d\sigma}{d\epsilon_p} = \frac{\alpha\mu Mb}{2\sqrt{\rho}} \frac{d\rho}{d\epsilon_p} + (\sigma - \sigma^*) \frac{d\ln\alpha}{d\epsilon_p}. \quad (4)$$

The change in  $\alpha$  is usually negligible for small strains. Thus finding the hardening rate requires an expression for  $d\rho/d\epsilon_p$ . The following sections are devoted to developing this expression.

(a)



(b)

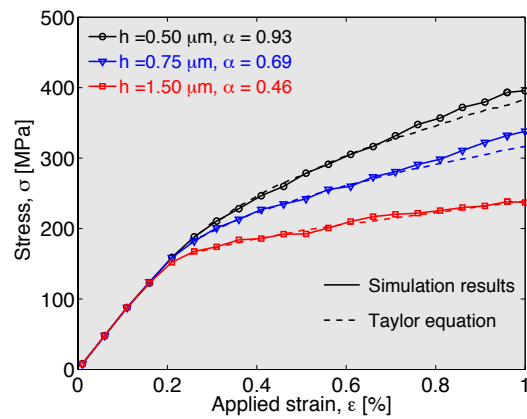


Figure 2: The stress-strain curves are plotted for three different film thicknesses  $h$  when dislocations (a) can only glide and (b) can glide and climb. Comparison between simulation and model shows that the Taylor equation is satisfied up for strains smaller than 0.7%.

## 4 Nucleation and Annihilation Rates

The Taylor equation provides a reasonable description of the flow stress of a material as a function of dislocation density. To be useful, however, the equation requires knowledge of how the dislocation density and structure evolves during plastic deformation of the material. In the absence of a free surface, the evolution of the dislocation density depends on two simultaneous mechanisms, dislocation nucleation and annihilation. This section is devoted to the derivation of relations that describe the generation and annihilation of dislocations. Simple expressions are developed and compared with simulation results.

### 4.1 Density of Active Sources

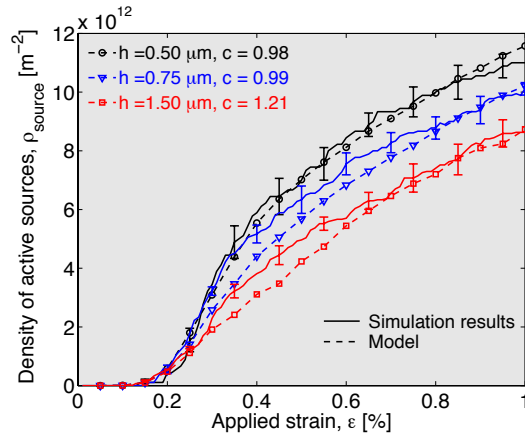
The dislocation nucleation rate is proportional to the density of active dislocation sources in a material; the higher the density of active sources, the higher is the generation rate. Here we evaluate the density of active sources as the stress in the film increases. Denote the distribution function that describes the strength of dislocation sources in a material by  $\phi(\tau)$ . If the resolved shear stress on a slip system is given by  $\tau_i$  and if we assume that the local shear stress is equal to the resolved shear stress, the probability that a source is active is given by the cumulative distribution function of the strength distribution  $\Phi(\tau_i)$ . If the number of sources on each slip system is approximately the same, the density of active sources  $\rho_{\text{source}}$  can be estimated as

$$\rho_{\text{source}} = c \sum_{i=1}^{N_{\text{slip system}}} \frac{\rho_{\text{source}}^0}{N_{\text{slip system}}} \Phi(\tau_i), \quad (5)$$

where  $N_{\text{slip system}}$  is the number of slip systems,  $\rho_{\text{source}}^0$  is the density of all dislocation sources (active or not) in the film, and  $c$  is a proportionality constant on the order of unity. In Eq. (5),  $\rho_{\text{source}}^0$  and  $N_{\text{slip system}}$  are fixed, the only variable is the resolved shear stress  $\tau_i$ . Figure 3 shows as a function of applied strain the density of active sources for three different DDD simulations. The same figure also shows the density of active dislocation sources determined from Eq. (5), where the resolved shear stress was determined from the average normal stress obtained in the simulations and where the proportionality constant was treated as a fitting parameter. The figure illustrates that the equation provides a good description of the active dislocation density and that the fitting parameters are all close to unity. The error in this approximation arises from three different sources: (1) Use of the strength distribution instead of the actual strength of a source introduces an error that decreases with increasing sample size and increased number of dislocation sources in the model. (2) The assumption that the number of sources is the same on each slip system also causes an error that decreases with a larger number of sources in the DDD model and thus better statistical

sampling. (3) The main error is probably arises from using the average normal stress to calculate the resolved shear stress instead of the local stress, which depends on the local dislocation configuration. These errors are captured by the proportionality constant  $c$  and cause the constant to deviate from unity. Even so, it is evident from Fig. (3) that Eq. (5) provides a good description of the density of active dislocation sources.

(a)



(b)

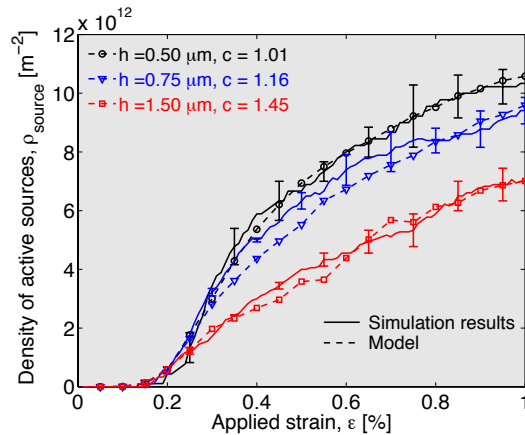


Figure 3: The solid curves denote the average density of active dislocation sources in the simulations for three different film thicknesses  $h$  when dislocations (a) can only glide or (b) can glide and climb. The dashed curves are the results of the procedure described in Section 4.1. Error bars show the standard error.

## 4.2 Dislocation Nucleation

An active dislocation source will emit a new dislocation whenever previously emitted dislocations have traveled far enough to decrease the back stress on the dislocation source. If that distance traveled is denoted by  $y_{\text{back}}$ , then the rate at which dislocations are generated is given by (Kocks et al., 1975)

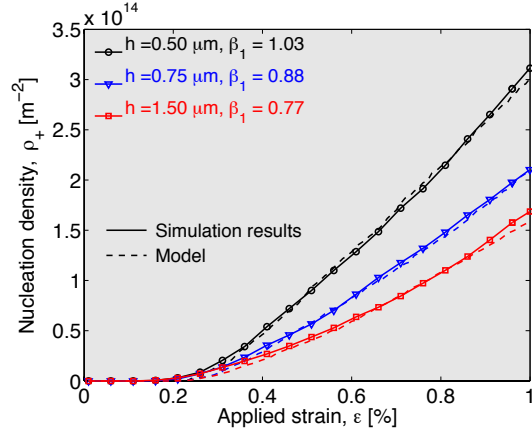
$$\frac{d\rho_+}{dt} = \rho_{\text{source}} \frac{\bar{v}}{y_{\text{back}}}. \quad (6)$$

Here  $\rho_{\text{source}}$  is the density of active sources,  $\bar{v}$  is the average dislocation velocity, which is related to the plastic shear strain rate by Orowan's equation  $\dot{\gamma}_p = \rho b \bar{v}$ . The travel distance  $y_{\text{back}}$  can be estimated by assuming a random distribution of dislocation sources, in which case  $y_{\text{back}}$  is proportional to  $\rho^{-1/2}$ . This assumption implies that the back stress on an active source must drop below the level of stress caused by randomly distributed dislocations (Kocks et al., 1975), before the source can emit another dislocation. The dislocation density in an annealed metal rises quickly after the material first becomes fully plastic. Consequently,  $\sqrt{\rho^*}$  is much smaller than  $\sqrt{\rho_Q}$  and, according to Eq. (2),  $y_{\text{back}}$  is inversely proportional to  $(\tau - \tau^*) / \mu b$ . In fact, the stresses induced by other dislocations are proportional to  $\alpha \rho^{1/2}$ , where  $\alpha$  can be taken as a constant as long as the strain is small. If we use  $(\tau - \tau^*) / \mu b$  instead, any change in  $\alpha$  due to dislocation pattern formations is automatically accounted for. Hence, Eq. (6) can be rewritten as

$$\frac{d\rho_+}{dt} = 2\pi\beta_1\rho_{\text{source}} \frac{\sigma - \sigma^*}{\rho\mu b^2} \frac{d\varepsilon_p}{dt}. \quad (7)$$

Figure 4 shows the density of the dislocation nucleation, i.e., the number of dislocation nucleations per unit area, versus applied strain obtained from the simulations, denoted by solid lines. The nucleation density can also be determined by integrating Eq. (7) using the stress, plastic strain, and dislocation density from the simulations and by considering  $\beta_1$  as a fitting parameter. The results are shown as the dashed curves in Fig. 4. Evidently Eq. (7) provides a very good description of the nucleation rate. When the dislocation density of a film is very low, the formula for  $y_{\text{back}}$  may yield a value that is larger than the film thickness or the grain size. It is then reasonable to assume that  $y_{\text{back}}$  is determined by geometry. This case was not observed in the simulations.

(a)



(b)

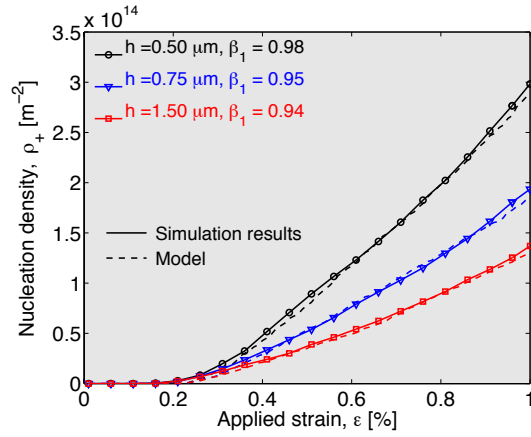


Figure 4: This figure shows how the dislocation density associated with nucleation,  $\rho_+$ , changes with applied strain, (a) for glide only and (b) for glide and climb. The solid lines were obtained from the simulations for three different film thicknesses  $h$ . The dashed lines were obtained from the model developed in this paper.

### 4.3 Dislocation Annihilation

The dislocation annihilation rate is inversely proportional to the mean free path before a dislocation encounters a dislocation of opposite sign. As the mean free path  $y_m$  decreases, the annihilation rate increases. Furthermore, the higher the dislocation density, the larger the chance of annihilation. Thus, the annihilation rate can be written as

$$\frac{d\rho_-}{dt} \propto \rho \frac{\bar{v}}{y_m}, \quad (8)$$

as suggested by Kocks et al. (1975). From geometry, the dislocation density and the mean free path are related through

$$\rho = \frac{1}{z_m y_m}, \quad (9)$$

where  $z_m$  is the average distance between dislocations in the direction perpendicular to the slip planes. Assuming that the active dislocation sources are randomly distributed,  $z_m^{-1}$  is proportional to  $2\sqrt{\rho_{\text{source}}}$ . Substituting these expressions into Eq. (8) and using Orowan's equation and the Taylor factor discussed in Section 3, the annihilation rate becomes

$$\frac{d\rho_-}{dt} = \beta_2 \frac{M\rho}{2b\sqrt{\rho_{\text{source}}}} \frac{d\varepsilon_p}{dt}, \quad (10)$$

where the Taylor factor has been used to convert shear rates into normal strain rates and where  $\beta_2$  is a dimensionless constant. At the onset of plastic deformation, the dislocation density is low and the assumption that  $y_m$  is proportional to  $2\sqrt{\rho_{\text{source}}}/\rho$  may yield a value that is larger than the length of the slip plane in very thin films. In this case, the mean free path is solely determined by geometry and may be taken proportional to the film thickness  $h$ . The annihilation rate then becomes

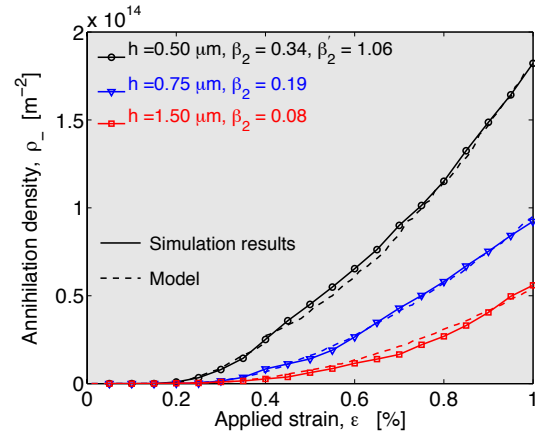
$$\frac{d\rho_-}{dt} = \frac{\beta'_2 M}{bh} \frac{d\varepsilon_p}{dt}, \quad (11)$$

where  $\beta'_2$  is another dimensionless constant. There may be different dislocation annihilation regimes during plastic deformation of very thin films. At the onset of plastic flow, Eq. (11) may be valid, but as more and more dislocations are generated, the mean free path decreases and Eq. (10) applies.

Figure 5 shows how the dislocation annihilation density, i.e., the number of dislocation annihilations per unit area, varies during plastic deformation of a thin film. The solid curves represent the annihilation density obtained from discrete dislocation simulations, while the dashed curves represent the results obtained from

the model – Eq. (10) in most cases; only for the thinnest film Eq. (11) had to be used for initial flow. The model provides a very good fit to the simulation results in all cases. The values of the  $\beta_2$  coefficients are quite small and decrease with increasing film thickness. This happens because only dislocations of opposite signs annihilate each other, and the distance between positive and negative dislocations becomes larger with increasing film thickness, thus reducing the probability of annihilation. The values of the coefficients also decrease when dislocation climb is enabled, primarily because climb tends to disperse dislocations decreasing the probability of annihilation. The value of  $\beta'_2$ , on the other hand, seems independent of whether dislocations climb, because dislocation climb only becomes significant at high stresses where the mean free path is smaller than the length of the slip planes in the films.

(a)



(b)

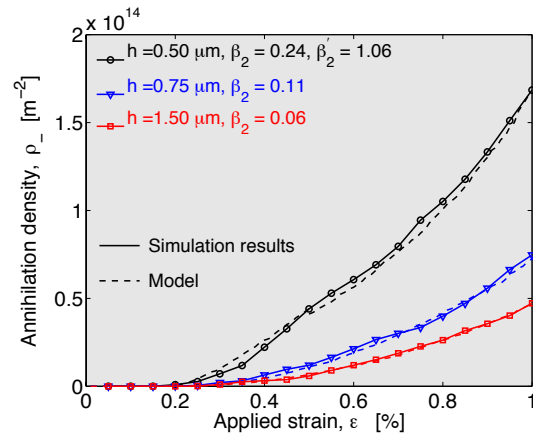


Figure 5: This figure shows how density of dislocation annihilation changes with the applied strain (a) for glide only and (b) for glide and climb. The solid lines were obtained from the simulations for three different film thicknesses  $h$ . The dashed lines are the results of the model presented in this paper.

## 4.4 Evolution of the dislocation density

The evolution of the dislocation density depends on both the dislocation nucleation and annihilation rates. Combining Eqs. (7) and (10), the rate of change of the dislocation density with respect to the plastic strain can be written as

$$\frac{d\rho}{d\varepsilon_p} = \frac{1}{\dot{\varepsilon}_p} \left( \frac{d\rho_+}{dt} - \frac{d\rho_-}{dt} \right) = 2\pi\beta_1\rho_{\text{source}} \frac{\sigma - \sigma^*}{\rho\mu b^2} - \beta_2 \frac{M\rho}{2b\sqrt{\rho_{\text{source}}}}. \quad (12)$$

If the mean free path of the dislocations is limited by the film thickness, the rate of change of the dislocation density is given by

$$\frac{d\rho}{d\varepsilon_p} = 2\pi\beta_1\rho_{\text{source}} \frac{\sigma - \sigma^*}{\rho\mu b^2} - \frac{\beta_2' M}{bh}. \quad (13)$$

Another length scale that may play a role in the governing equation is the spacing of obstacles in the film. In general, obstacles may be precipitates or immobile dislocations, and may result in the formation of pile-ups that increase the flow stress of the material. The hardening effect of obstacles is governed by the density and strength of obstacles (Roos et al., 2001; Chakravarthy and Curtin, 2010). If the density of obstacles is large, the mean free paths  $y_m$  and  $y_{\text{back}}$  may be limited by obstacle spacing and Eqs. (12) or (13) may need to be modified.

Experiments and calculations (Xiang and Vlassak, 2005, 2006; Nicola et al., 2006) demonstrate that the absence of passivation layers lowers the flow stress and hardening rate. If the surfaces of a film are not passivated, dislocations can escape from the film and a term that accounts for dislocations leaving the film needs to be subtracted from the right hand sides of Eqs. (12) or (13). This term is similar to the expression developed by Nix and Lee (2011) for the rate of dislocations leaving micropilars, and is inversely proportional to the film thickness.

As plastic flow proceeds, the dislocation density rises and the number of active sources increases. If the film contains a finite number of dislocation sources,  $\rho_{\text{source}}$  will approach the total density of sources and eventually the right hand side of Eq. (12) will vanish: The evolution equation has an asymptote and the normal stress saturates, provided the Taylor equation still holds true. This behavior is observed in some experiments on bulk materials at high temperatures (see, e.g., Kocks, 1976) and in many simulations if the initial density of sources is high or the grains are relatively large (see, e.g., Balint et al., 2008). Higher temperatures, a high density of initial sources, and large grains ensure the validity of the Taylor equation with a constant coefficient. At high temperatures, dislocations become more dispersed; large grains delay the formation of pile-ups, and a high density of sources increases the interactions of dislocations on different slip planes compared to the interactions of

dislocations on the same slip planes. When these conditions are met, the hardening rate decreases and the stress may reach a saturation stress.

In this study, we considered a fixed number of dislocation sources. In three-dimensional problems, junctions form when two dislocations on different slip planes intersect. These junctions can restrict the motion of dislocations, provide pinning points, and act as new Frank-Read sources. It is then reasonable to assume that the density of active sources is proportional to the dislocation density (Kocks et al., 1975). If we insert  $\rho_{\text{source}} \propto \rho$  into Eq. (12), we arrive at the deterministic evolution equation of the total dislocation density proposed by Hähner (1996b).

The evolution equation developed in this paper contains two constants that need to be determined from experiments or simulations. Since dislocations do not leave the surface in the model considered here, the evolution equation can also be applied to bulk materials. Thus it may be possible to determine these parameters from measurements performed on bulk materials. Alternately the parameters may be determined at the micro-scale using DDD simulations and then used in a multi-scale model for bulk materials.

## 5 Conclusions

We have employed discrete dislocation dynamics to develop a dislocation evolution equation that contains just two parameters. Discrete dislocation simulations show that the Taylor equation is well satisfied as long as dislocations are more or less randomly distributed and no substructure is formed. Once significant dislocation pile-ups form, stress-strain curves deviate from the Taylor equation. Expressions have been developed for the density of active dislocation sources, the rate of dislocation nucleation, and the rate of dislocation annihilation. For low dislocation densities and very thin films, these expressions may change because of geometrical considerations. Comparison between the discrete dislocation simulations and the models reveals very good agreement. With the aid of these expressions, we have developed a dislocation evolution equation that contains just two parameters.

## Acknowledgment

The authors gratefully acknowledge support from NSF (Grant DMR-0820484). The authors wish to thank Professor Lucia Nicola of Delft University for the help with the DDD simulation code and for insightful discussions.

## References

- Aifantis, E.C., 1986. On the Dynamical Origin of Dislocation Patterns. *Mater. Sci. Eng.* 81, 563–574.
- Balint, D.S., Deshpande, V.S., Needleman, A., Van der Giessen, E., 2008. Discrete dislocation plasticity analysis of the grain size dependence of the flow strength of polycrystals. *Int. J. Plast.* 24, 2149–2172.
- Chakravarthy, S.S., Curtin, W. a., 2010. Effect of source and obstacle strengths on yield stress: A discrete dislocation study. *J. Mech. Phys. Solids* 58, 625–635.
- Cottrell, A.H., 2002. Commentary. A brief view of work hardening, in: *Dislocations in Solids* 11. Elsevier B.V., pp. vii–xvii.
- Danas, K., Deshpande, V.S., 2013. Plane-strain discrete dislocation plasticity with climb-assisted glide motion of dislocations. *Model. Simul. Mater. Sci. Eng.* 21, 045008.
- Davoudi, K.M., Nicola, L., Vlassak, J.J., 2012. Dislocation climb in two-dimensional discrete dislocation dynamics. *J. Appl. Phys.* 111, 103522.
- Davoudi, K.M., Nicola, L., Vlassak, J.J., 2014. Bauschinger effect in thin metal films: Discrete dislocation dynamics study. *J. Appl. Phys.* 115, 013507.
- De Guzman, M.S., Neubauer, G., Flinn, P., Nix, W.D., 1993. The role of indentation depth on the measured hardness of materials. *Mater. Res. Soc. Symp. Proc* 308, 613–618.
- Devincre, B., Hoc, T., Kubin, L.P., 2008. Dislocation mean free paths and strain hardening of crystals. *Science* 320, 1745–8.
- Doerner, M., Nix, W.D., 1986. A method for interpreting the data from depth-sensing indentation instruments. *J. Mater. Res.* 1, 601–609.
- El-Awady, J. a., Rao, S.I., Woodward, C., Dimiduk, D.M., Uchic, M.D., 2011. Trapping and escape of dislocations in micro-crystals with external and internal barriers. *Int. J. Plast.* 27, 372–387.
- Estrin, Y., 1996. Dislocation-Density-Related Constitutive Modeling, in: *Unified Constitutive Laws of Plastic Deformation*, (Eds. AS Krausz and K. Krausz). Academic Press, pp. 69–106.
- Estrin, Y., Mecking, H., 1984. A unified phenomenological description of work hardening and creep based on one-parameter models. *Acta Metall.* 32, 57–70.

- Fleck, N.A., Muller, G., Ashby, M.F., Hutchinson, J.W., 1994. Strain Gradient Plasticity: Theory and Experiment. *Acta Metall. Mater.* 42, 475–487.
- Follansbee, P.S., Kocks, U.F., 1988. A constitutive description of the deformation of copper based on the use of the mechanical threshold stress as an internal state variable. *Acta Metall.* 36, 81–93.
- Friedel, J., 1955. On the linear work hardening rate of face-centred cubic single crystals. *Philos. Mag. Ser. 7* 46, 1169–1186.
- Gómez-García, D., Devincre, B., Kubin, L.P., 2006. Dislocation Patterns and the Similitude Principle: 2.5D Mesoscale Simulations. *Phys. Rev. Lett.* 96, 8–11.
- Greer, J.R., Weinberger, C., Cai, W., 2008. Comparing the strength of f.c.c. and b.c.c. sub-micrometer pillars: Compression experiments and dislocation dynamics simulations. *Mater. Sci. Eng. A* 493, 21–25.
- Groh, S., Marin, E.B., Horstemeyer, M.F., Zbib, H.M., 2009. Multiscale modeling of the plasticity in an aluminum single crystal. *Int. J. Plast.* 25, 1456–1473.
- Guruprasad, P.J., Benzerga, a. A., 2008. Size effects under homogeneous deformation of single crystals: A discrete dislocation analysis ☆. *J. Mech. Phys. Solids* 56, 132–156.
- Hähner, P., 1996a. On the foundations of stochastic dislocation dynamics. *Appl. Phys. A Mater. Sci. Process.* 62, 473–481.
- Hähner, P., 1996b. A theory of dislocation cell formation on stochastic dislocation dynamics based. *Acta Mater.* 44, 2345–2352.
- Hall, E.O., 1951. The deformation and ageing of mild steel: III discussion of results. *Proc. Phys. Soc. Sect. B* 64, 747–753.
- Hillert, M., Ågren, J., 2006. Extremum principles for irreversible processes. *Acta Mater.* 54, 2063–2066.
- Hirsch, P.B., 1959. Internal stresses and fatigue in metals, in: *General Motors Symposium*. Elsevier, Amsterdam, p. 159.
- Hirsch, P.B., Mitchell, T., 1967. Stage II work hardening in crystals. *Can. J. Phys.* 45, 663–706.
- Hirth, J.P., Lothe, J., 1982. *Theory of dislocations*, 2nd ed. John Wiley & Sons.
- Hull, D., Bacon, D.J., 2011. *Introduction to dislocations*, 5th ed. Elsevier.

- Ispánovity, P.D., Groma, I., Györgyi, G., Csikor, F.F., Weygand, D., 2010. Submicron Plasticity: Yield Stress, Dislocation Avalanches, and Velocity Distribution. *Phys. Rev. Lett.* 105, 085503.
- Ispánovity, P.D., Hegyi, Á., Groma, I., Györgyi, G., Ratter, K., Weygand, D., 2013. Average yielding and weakest link statistics in micron-scale plasticity. *Acta Mater.* 61, 6234–6245.
- Kocks, U.F., 1970. The relation between polycrystal deformation and single-crystal deformation. *Metall. Mater. Trans.* 1, 1121–1143.
- Kocks, U.F., 1976. Laws for Work-Hardening and Low-Temperature Creep. *J. Eng. Mater. Technol.* 98, 76–85.
- Kocks, U.F., Argon, A.S., Ashby, M.F., 1975. Thermodynamics and kinetics of slip, *Progr. Mater. Sci.* Pergamon Press Ltd.
- Kocks, U.F., Mecking, H., 1980. Dislocation kinetics at not-so-constant structure, in: Bullough, R., Wells, D.W., Willis, J.R., Wood, M.H., Ashby, M.F., Hartley, C.S., Hirth, J.P. (Eds.), *Dislocation Modelling of Physical Systems*. Pergamon Press Ltd., pp. 173–192.
- Kocks, U.F., Mecking, H., 2003. Physics and phenomenology of strain hardening: the FCC case. *Prog. Mater. Sci.* 48, 171–273.
- Kubin, L., Devincere, B., Hoc, T., 2009. The deformation stage II of face-centered cubic crystals: Fifty years of investigations. *Int. J. Mater. Res.* 100, 1411–1419.
- Kubin, L.P., Canova, G., 1992. The modelling of dislocation patterns. *Scr. Metall. Mater.* 27, 957–962.
- Kubin, L.P., Canova, G., Condat, M., Devincere, B., Pontikis, V., Bréchet, Y., 1992. Dislocation Microstructures and Plastic Flow: A 3D Simulation. *Solid State Phenom.* 23, 455–472.
- Kuhlmann-wilsdorf, D., 1962. A new theory of workhardening, in: *Trans. Met. Soc. AIME*. pp. 1047–1061.
- Kuhlmann-Wilsdorf, D., 1985. Theory of workhardening 1934-1984. *Metall. Trans. A* 16a, 2091–2108.
- Kumar, R., Nicola, L., Van der Giessen, E., 2009. Density of grain boundaries and plasticity size effects: A discrete dislocation dynamics study. *Mater. Sci. Eng. A* 527, 7–15.
- Lavrentev, F., 1980. The type of dislocation interaction as the factor determining work hardening. *Mater. Sci. Eng.* 46, 191–208.

- Lee, S.-W., Jennings, A.T., Greer, J.R., 2013. Emergence of enhanced strengths and Bauschinger effect in conformally passivated copper nanopillars as revealed by dislocation dynamics. *Acta Mater.* 61, 1872–1885.
- Leibfried, G., 1951. Verteilung von Versetzungen. *Zeitschrift für Phys.* 130, 214–226.
- Lloyd, D.J., 1994. Particle reinforced aluminium and magnesium matrix composites. *Int. Mater. Rev.* 39, 1–23.
- Ma, Q., Clarke, D.R., 1995. Size dependent hardness of silver single crystals. *J. Mater. Res.* 10, 853–863.
- Madec, R., Devincere, B., Kubin, L.P., 2002. From Dislocation Junctions to Forest Hardening. *Phys. Rev. Lett.* 89, 255508.
- Mader, S., Seeger, A., Thieringer, H.-M., 1963. Work Hardening and Dislocation Arrangement of fcc Single Crystals. II. Electron Microscope Transmission Studies of Ni[Single Bond]Co Single Crystals and Relation to Work-Hardening Theory. *J. Appl. Phys.* 34, 3376–3386.
- McElhaney, K.W., Vlassak, J.J., Nix, W.D., 1998. Determination of indenter tip geometry and indentation contact area for depth-sensing indentation experiments. *J. Mater. Res.* 13, 1300–1306.
- Mecking, H., Kocks, U.F., 1981. Kinetics of flow and strain-hardening. *Acta Metall.* 29, 1865–1875.
- Miguel, M., Vespignani, A., Zapperi, S., 2001. Intermittent dislocation flow in viscoplastic deformation. *Nature* 410, 667–671.
- Nabarro, F.R.N., Basinski, Z., Holt, D., 1964. The plasticity of pure single crystals. *Adv. Phys.* 13, 193–323.
- Nicola, L., Xiang, Y., Vlassak, J.J., Van der Giessen, E., Needleman, A., 2006. Plastic deformation of freestanding thin films: Experiments and modeling. *J. Mech. Phys. Solids* 54, 2089–2110.
- Nix, W.D., Lee, S.-W., 2011. Micro-pillar plasticity controlled by dislocation nucleation at surfaces. *Philos. Mag.* 91, 1084–1096.
- Petch, N.J., 1953. The cleavage strength of polycrystals. *J. Iron Steel Inst.* 174, 25–28.
- Poole, W.J., Ashby, M.F., Fleck, N.A., 1996. micro-hardness of annealed and work-hardened copper polycrystals. *Scr. Mater.* 34, 559–564.

- Rice, J., 1987. Tensile crack tip fields in elastic-ideally plastic crystals. *Mech. Mater.* 6, 317–335.
- Roos, A., De Hosson, J.T.M., Van der Giessen, E., 2001. A two-dimensional computational methodology for high-speed dislocations in high strain-rate deformation. *Comput. Mater. Sci.* 20, 1–18.
- Ryu, I., Nix, W.D., Cai, W., 2013. Plasticity of bcc micropillars controlled by competition between dislocation multiplication and depletion. *Acta Mater.* 61, 3233–3241.
- Sauzay, M., Kubin, L.P., 2011. Scaling laws for dislocation microstructures in monotonic and cyclic deformation of fcc metals. *Prog. Mater. Sci.* 56, 725–784.
- Seeger, A., 1955. CXXXII. The generation of lattice defects by moving dislocations, and its application to the temperature dependence of the flow-stress of FCC crystals. *Philos. Mag.* 46, 1194–1217.
- Seeger, A., Diehl, J., Mader, S., Rebstock, H., 1957. Work-hardening and work-softening of face-centred cubic metal crystals. *Philos. Mag.* 2, 323–350.
- Shishvan, S.S., Mohammadi, S., Rahimian, M., Van der Giessen, E., 2011. Plane-strain discrete dislocation plasticity incorporating anisotropic elasticity. *Int. J. Solids Struct.* 48, 374–387.
- Shishvan, S.S., Nicola, L., Van der Giessen, E., 2010. Bauschinger effect in unpassivated freestanding thin films. *J. Appl. Phys.* 107, 093529.
- Stelmashenko, N.A., Walls, M.G., Brown, L.M., Milman, Y. V., 1993. microindentation on W and Mo Oriented single crystals: an STM study. *Acta Metall. Mater.* 41, 2855–2865.
- Stölken, J., Evans, A., 1998. A microbend test method for measuring the plasticity length scale. *Acta Mater.* 46, 5109–5115.
- Taylor, G.I., 1934. The Mechanism of Plastic Deformation of Crystals. Part I.-Theoretical. *Proc. R. Soc. London. Ser. A, Contain. Pap. a Math. Phys. Character* 145, 362–387.
- Turner, A.P.L., 1979. Cyclic deformation behavior of type 304 stainless steel at elevated temperature. *Metall. Trans. A* 10, 225–234.
- Uchic, M.D., Dimiduk, D.M., Florando, J.N., Nix, W.D., 2004. Sample dimensions influence strength and crystal plasticity. *Science* (80-. ). 305, 986–989.

- Van der Giessen, E., 2010. Discrete Dislocation Plasticity Analysis of Cracks and Fracture, in: *Multiscale Modelling of Plasticity and Fracture by Means of Dislocation Mechanics*. Springer, pp. 185–212.
- Van der Giessen, E., Needleman, A., 1995. Discrete dislocation plasticity : a simple planar model. *Model. Simul. Mater. Sci. Eng.* 3, 689–735.
- Viguier, B., 2003. Dislocation densities and strain hardening rate in some intermetallic compounds. *Mater. Sci. Eng. A* 349, 132–135.
- Walgraef, D., Aifantis, E.C., 1985a. On the formation and stability of dislocation patterns -I: one-dimensional considerations. *Int. J. Eng. Sci.* 23, 1351–1358.
- Walgraef, D., Aifantis, E.C., 1985b. On the formation and stability of dislocation patterns -II: two-dimensional considerations. *Int. J. Eng. Sci.* 23, 1359–1364.
- Walgraef, D., Aifantis, E.C., 1985c. On the formation and stability of dislocation patterns -III: three-dimensional considerations. *Int. J. Eng. Sci.* 23, 1365–1372.
- Xiang, Y., Vlassak, J.J., 2005. Bauschinger effect in thin metal films. *Scr. Mater.* 53, 177–182.
- Xiang, Y., Vlassak, J.J., 2006. Bauschinger and size effects in thin-film plasticity. *Acta Mater.* 54, 5449–5460.
- Xiang, Y., Vlassak, J.J., Perez-Prado, M.T., Tsui, T.Y., McKerrow, A.J., 2004. freestanding electroplated Cu thin films with constant microstructure. *Mater. Res. Soc. Symp. Proceeding* 795, 417–422.